Multi-Layer Arctic Mixed-Phase Clouds Simulated by a Cloud-Resolving Model: Comparison with ARM Observations and Sensitivity Experiments

Contact: yali@cams.cma.gov.cn

Yali Luo [1], Kuan-Man Xu [2], Hugh Morrison[3], Greg M. McFarquhar[4], Zhien Wang[5], and Gong Zhang[4]

[1] State Key Laboratory of Severe Weather, Chinese Academy of Meteorological Sciences, Beijing, China; [2] NASA Langley Research Center, Hampton, VA, USA; [3] National Center for Atmospheric Research, Boulder, CO, USA; [4] University of Illinois at Urbana-Champaign, Urbana, IL, USA; [5] University of Wyoming, Laramie, WY, USA

1. Introduction

Arctic clouds have been identified as playing a central role in the Arctic climate system that has been changed significantly in the recent decades and can potentially impact global climate. A few field campaigns have been conducted to improve the understanding of cloud-radiative interactions in the Arctic. These field campaigns identified that mixed-phase stratiform (MPS) clouds were prevalent in Arctic transition seasons, especially during the fall over Barrow at the Atmospheric Radiation Measurement (ARM) North Slope of Alaska (NSA) site. This type of mixed-phase cloud is a water-dominated cloud layer with precipitating ice, yet they persist for long periods of time.

The U.S. DOE ARM Program conducted its M-PACE field campaign over the NSA during the period of 27 September - 22 October 2004. During the field campaign, Arctic clouds were measured in detail using a wide range of instruments such as the ARM millimeter wavelength cloud radar (MMCR), micropulse lidar (MPL), laser ceilometers, and two instrumented aircraft. ARM has also derived the Cloud Resolving Model (CRM) / Single-Column Model (SCM) forcing data from a sounding network in the Arctic region for a seventeen and half day Intensive Operational Period in October 2004.

Despite the rapid progress in the understanding of single-layer Arctic mixed-phase clouds through modeling studies, multi-layer Arctic MPS are seldom modeled. The present modeling study attempts to increase the understanding of physical mechanisms for the formation and maintenance of multi-layer Arctic mixed-phase clouds. The objectives of this study are twofold. The first objective is to examine how well the University of California at Los Angeles / Chinese Academy of Meteorological Sciences (UCLA/CAMS) CRM simulates the occurrences and evolution of the multiple-layer MPS clouds and their complex macroscopic and microphysical structures. The second goal is to explore the possible mechanisms for the formation, maintenance, and decay of the multiple-layer MPS clouds.

2. Field measurements

2.1 Large-scale environment

The NSA was under three different synoptic regimes with two transition periods during M-PACE (Verlinde et al. 2007). This study focuses on a three-and-a-half-day subperiod (14Z 5 October to 02Z 9 October) of the second regime (between 4 and 13 October). This synoptic regime was featured by high pressure building over the pack ice to the northeast of the Alaska coast (Fig. 1). As the high pressure system dominated the NSA until 15 October, a small midlevel low pressure system drifted along the northern Alaska coast from 5 to 7 October, and dissipated between Deadhorse and Barrow on 7 October. This midlevel low brought a considerable amount of mid- and upper-level moisture to the NSA. The low-level northeasterly flow out of the high pressure and the small midlevel disturbance related to the low pressure system combined to produce a complicated multilayer cloud structure over the NSA.

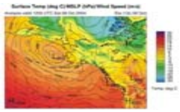

Figure 1. ETA analysis for 1200 UTC 09 October 2004. Shown are temperatures (shaded), mean sea level pressure (contoured) and windbarbs.

2.2 Cloud properties

Clouds were observed by a wide range of instruments, which were deployed at the ARM NSA surface sites (Barrow, Oliktok Point and Atqasuk; Figure 2) or aboard the two aircraft participated in the M-PACE. The University of North Dakota (UND) Citation served as an in situ platform. Cloud properties are derived from these surface and air-based measurements. Liquid water path (LWP) and precipitable water vapor were derived from the 2-channel (23.8 and 31.4 GHz) microwave radiometers (MWRs) deployed at the ARM NSA surface sites (Turner et al., 2007).

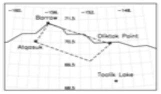

Figure 2. The area of the M-PACE campaign. Asterisks are the locations of the sounding stations. Sounding data are used to derive large-scale forcing data over the area enclosed by dashed lines. The latitudes and longitudes are represented by dotted lines and the solid line represents the coastline.

Occurrences and locations of mixed-phase cloud layers

Occurrences of the mixed-phase cloud layers, along with their base and top heights, were determined by combining measurements from the MPL (Micropulse Lidar) and MMCR (Millimeter Wavelength Cloud Radar) deployed at Barrow. These measurements were available at a time interval of ~35 s. The vertical resolution of the MMCR is ~45 m and that of the MPL is ~30 m.

Bulk cloud microphysical properties

The bulk microphysical properties of the multiple-layer MPS clouds were derived from the UND Citation measurements on October 5, 6, and 8. The properties used in the present study include liquid water content (LWC), total ice water content (IWC), total water droplet number concentration (n_c), and total ice crystal number concentration (n_{ti}). The bulk properties are available at a 10 s interval, but represent a 30 s running average of the measured ice properties. There are 628, 829, and 289 in-cloud observations obtained during the three missions, respectively, covering a total in-cloud period of about five hours. The numbers of the samples of LWC and IWC within each of the 400 m height bin are represented in Figure 3.

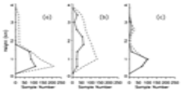

Figure 3. Profiles of the sample numbers for liquid water content (solid lines) and ice water content (dashed lines), respectively, in each height bin of 400 m during the three missions that the UND Citation took on October 5 (a), October 6 (b), and October 8 (c), 2004.

2.3 Aerosol properties

Aerosol size distribution and chemical composition are needed for the calculation of droplet activation in the CRM simulations. Ice nuclei (IN) concentration is needed for the purpose of calculating heterogeneous ice nucleation in the CRM.

A bimodal lognormal aerosol size distribution (Fig. 4) was fitted to the average size-segregated Hand-Held Particle Counter (HHPC-6) measurement on October 10, with the total aerosol concentration constrained by the average NOAA Earth System Research Laboratory condensation nuclei measurements.

The measurements of active IN concentration represent the sum of IN acting in deposition, condensation-freezing, and immersion-freezing modes. The observed mean IN number concentration (0.16 L^{-1}) is used in our CRM simulations to represent the aforementioned nucleation modes. The contact IN number is a function of temperature following Meyers et al. (1992).

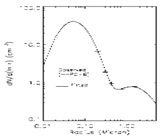

Figure 4. Observed and fitted dry aerosol size distribution.

3. Numerical simulations

3.1 Model

The model used in this study is the University of California at Los Angeles / Chinese Academy of Meteorological Sciences (UCLA/CAMS) cloud-resolving model (CRM). The CRM is based on the anelastic dynamic framework in 2 dimensions (x and z) with a third-order turbulence closure (Krueger 1988). The two-moment microphysics scheme of Morrison et al. (2005) and the radiative transfer scheme of Fu and Liou (1993) are coupled to the dynamic framework (Luo et al., 2008a).

3.2 Large-scale forcing data

The large-scale forcing data used to drive the CRM are shown in Fig. 5 (right). Panels (a) and (b) represent the time-pressure cross sections of the large-scale advective tendencies of temperature and water vapor mixing ratio, respectively. The hatched areas in panel (a) represent warming (cooling) rates larger than 4 K day^{-1} and in panel (b) represent moistening (drying) rates larger than 2 g kg^{-1} day^{-1}. Panel (c) represents the time-series of the surface turbulent fluxes of latent heat (solid line) and sensible heat (dashed line) with the labels "A", "B" and "C" indicating the periods of the Citation missions taken on October 5, 6, and 8, respectively. Panel (d) shows the spectral albedo over fresh snow corresponding to a broadband albedo of 0.86 for the six shortwave bands of the Fu and Liou (1993) radiative transfer scheme.

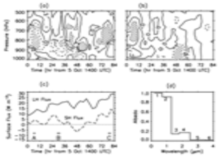

Figure 5.

3.3 Sensitivity experiments

Eight numerical experiments are performed, including the Baseline simulation and seven sensitivity studies (Table 1). The sensitivity simulations consist of noLSadv, noSfcFlx, noLWrad, noIce, IN5th, IN5 and noMicLat simulations, which are identical to the Baseline simulation except that one aspect of the experimental designs is artificially altered.

Table 1. A list of simulations performed in this study.

Simulation	Description
Baseline	Standard baseline simulation
noSfcFlx	Neglecting surface turbulent fluxes of latent and sensible heat
noLSforcing	Neglecting large-scale advective forcing
noLWrad	Neglecting longwave radiative cooling/heating
noIce	Neglecting ice-phase microphysical processes
IN50	Increasing ice-forming nuclei concentration from 0.16 L^{-1} to 8.0 L^{-1}
IN50th	Decreasing ice-forming nuclei concentration from 0.16 L^{-1} to 0.003 L^{-1}
noMicLat	Neglecting cooling/heating caused by phase changes of hydrometeors

4. Baseline results

4.1 Temperature, moisture, and surface precipitation

The atmospheric temperature and water vapor mixing ratio (q_v) decrease with height from nearly 0°C and ~ 4 g kg^{-1} at the surface to –24°C and 0.5 g kg^{-1} at ~ 500 hPa (~ 4.7 km) in the Baseline simulation (Figs. 6a and 6b). Typical differences in temperature between the Baseline simulation and the ARM analysis are between –2°C and +2°C and those in q_v are between -0.25 g kg^{-1} and 0.25 g kg^{-1}. There are larger differences within the 850-700 hPa layer, i.e., cold (dry) biases up to -4 K (-0.5 g kg-1) before 48 h and opposite biases of the same magnitudes after 48 h (Figs. 6c and 6d). A primary reason for the large T biases is the unreasonable partitioning of ice water content (IWC) and liquid water content (LWC). IWC is underestimated and LWC is probably overestimated between 12-24 h in the simulation, resulting in extra radiative cooling (Fig. 11b) and negative T biases near the cloud tops, as evidenced by the elevation of negative T biases with time during the first 48 h. This is due to the fact that optical properties of ice crystals and water droplets differ greatly for the same amount of ice/water. The large dry biases are unlikely caused by microphysical drying, as the surface precipitation is underestimated (Fig. 6e). One possible cause is that the moistening associated with the midlevel low is underestimated in the large-scale forcing data. The positive biases in T and qv after 48 h may be related to the underestimation in clouds and precipitation during 44-60 h.

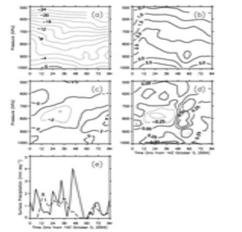

Figure 6. Time-pressure cross sections of temperature (a) and water vapor mixing ratio (b) from the Baseline simulation, and their differences from the ARM analysis in temperature (c) and water vapor mixing ratio (d). Panel (e) shows the time-series of surface precipitation rate from the M-PACE observations (solid line) and the Baseline simulation (dashed line).

4.2 Cloud properties

Occurrences of multiple-layer MPS clouds

One of the unique features of the Arctic MPS clouds under study is that there are multiple mixed-phase cloud layers coexisting. Statistics of their occurrences are computed using the MMCR-MPL observations at Barrow. To compare with the observations, the number of mixed-phase cloud layers at each individual CRM grid column, as well as the base and top heights of the cloud layers, is determined by analyzing the profiles of cloud water mixing ratio (q_c) and cloud ice plus snow mixing ratio (q_{is}) at a 5-min temporal interval from the Baseline simulation.

The results in Table 2 (below) suggest that the Baseline simulation reasonably reproduced the occurrences of the multiple-layer MPS clouds as revealed by the statistics of MMCR-MPL observations.

	1- layer	2-layer	3-layer	1- layer (%)	2-layer (%)	3-layer (%)
MMCR-MPL 10.06	1186	997	206	49	41	9
CRM 12-36 h	10574	23825	2584	29	64	7
MMCR-MPL 10.07	1532	721	70	66	31	3
CRM 36-60 h	13137	7574	139	63	36	1
MMCR-MPL 10.08	2010	225	8	90	10	0
CRM 60-84 h	23584	12381	9	66	34	0
MMCR-MPL 10.06	4728	1943	284	68	28	4
CRM 12-84 h	47295	43780	2732	50	47	3

Mixed-phase cloud layer boundaries

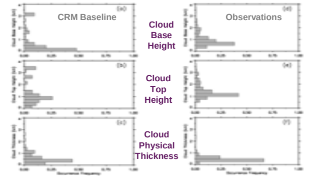

Figure 7. Histograms of base height (a and d), top height (b and e), and physical thickness (c and f) of the first mixed-phase cloud layer above the surface from the Baseline simulation (left column) and the MMCR-MPL observations at Barrow (right column).

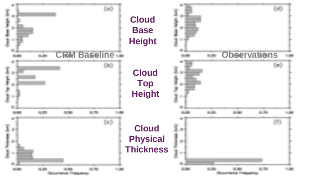

Figure 8. Similar to Figure 7, except for the second mixed-phase cloud layer above the surface.

The bases and tops of the simulated lower MPS cloud layer (Fig. 7) are too low and the physical thicknesses of the simulated upper MPS cloud layer (Fig. 8) appear too large.

Liquid Water Path (LWP)

The 78hr- and domain-averaged Baseline LWP is about the same as the MWR-based LWP averaged at the three sites (79 g m^{-2} versus 81 g m^{-2}). However, the temporal variations of the simulated and retrieved 3-hourly averaged LWPs are different (Fig. 9). The simulated LWP decreases with time from 12 h to 48 h and increases at ~ 60 h. The retrieved LWP, when averaged among the three sites, is relatively more constant with time. It is likely that the retrievals averaged among the three sites may not represent the evolution of the domain-averaged LWP. The retrieved LWPs at the three sites not only differ in the 78-hr-averaged values: 124 g m-2 at Barrow, 61 g m-2 at Oliktok Point, and 57 g m-2 at Atqasuk, but also evolve with distinct patterns.

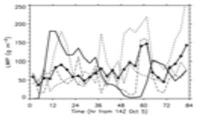

Figure 9. Time series of 3-hourly averaged liquid water path (LWP) produced by the Baseline simulation averaged over the CRM domain (thick solid line without symbols) and derived from the microwave radiometer (MWR) measurements averaged over the DOE-ARM NSA sites (thick solid line with diamonds). The thin lines represent the MWR LWPs at Barrow (short dashed line), Atqasuk (dash-dotted line) and Oliktok Point (long dashed line), respectively.

Bulk cloud microphysical properties

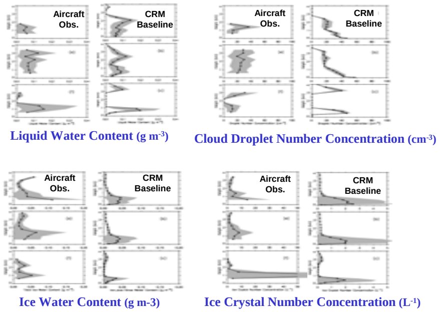

Figure 10. Vertical profiles of LWC, n_c, total IWC, and total n_{ti} from the Baseline simulation (a-c) and from the Citation measurements (d-f).

The Baseline simulation qualitatively captured the major characteristics in the vertical distributions of LWC, nc, ISWC and nis and their interperiod differences suggested by the aircraft observations(Fig. 10). However, nc within the lower layer decreases with height, in contrast to the relatively constant nc revealed by the observations. This could be due to uncertainties associated with the parameterizations, surface fluxes, and/or radiation. The second cloud layer is physically too thick with too large LWC, causing too strong LW cooling and negative biases in temperature. Both cloud layers contain too few ice crystal numbers and too small ice crystal masses.

5. Results from sensitivity experiments

The sensitivity experiments show that both the surface fluxes and large-scale advective forcing control the formation of the lower cloud layer while the large-scale advective forcing initiates the formation of the upper cloud layer but maintenance of multi-layer structures relies on the LW radiative effect, which favors condensation in the upper cloud layer through cloud-top cooling and creates the stability gap between the two cloud layers through cloud-base warming of the upper layer. Moreover, ice crystals consume cloud liquid droplets through the Bergeron-Findeisen mechanism and remove condensate from the cloud layer through precipitation. Therefore, without large-scale advection, which re-supplies moisture, and cloud-top LW cooling, which produces a more saturated environment, the upper cloud layer will dissipate. Furthermore, both the upper and lower mixed-phase cloud layers are very sensitive to IFN concentration because of the Bergeron-Findeisen mechanism. Finally, the microphysical changes, which feed into the LW radiative cooling, could significantly influence the mesoscale circulation that helps maintain the cloud layer.

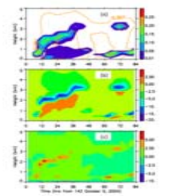

Figure 11. Time-height cross section of 3-hourly and horizontally averaged (a) liquid water content (color shades) and ice plus snow water content (lines) (unit: g m^{-3}), (b) LW radiative cooling (negative) rates, and (c) heating rates caused by microphysical processes from the Baseline simulation. The unit of the color bars in (b) and (c) is K day^{-1}.

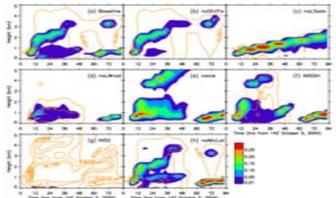

Figure 12. Time-height cross sections of 3-hourly and horizontally-averaged liquid water content (color shades) and ice plus snow water content (lines) from the (a) Baseline, (b) noSfcFlx, (c) noLSadv, (d) noLWrad, (e) noIce, and (f) IN50th, (g) IN50 and (h) noMicLat experiments. See Table 1 for explanations about the experiments.

6. Summary

A cloud-resolving model (CRM) is used to simulate the multiple-layer mixed-phase stratiform (MPS) clouds that occurred during a three-and-a-half day subperiod of the Department of Energy-Atmospheric Radiation Measurement Program's Mixed-Phase Arctic Cloud Experiment (M-PACE) and to examine physical processes responsible for multi-layer production and evolution. The CRM with a two-moment cloud microphysics is initialized with concurrent meteorological, aerosol, and ice nucleus measurements and is driven by time-varying large-scale advective tendencies of temperature and moisture and surface sensible and latent heat fluxes.

The CRM reproduces the dominant occurrences of the single- and double-layer MPS clouds as revealed by the M-PACE observations although the simulated first cloud layer is lower and the second cloud layer is thicker compared to observations. The aircraft measurements suggest that the CRM qualitatively captures the major characteristics in the vertical distribution and interperiod variation of liquid water content (LWC), droplet number concentration, total ice water content (IWC) and ice crystal number concentration (nis). However, the magnitude of LWC is overestimated and those of IWC and nis are underestimated. In particular, the simulated nis is one order of magnitude smaller than the observed.

Sensitivity experiments suggest that both the surface fluxes and large-scale advection control the formation of the lower cloud layer while the large-scale advection initiates the formation of the upper cloud layer but the maintenance of multi-layer structures relies on the longwave (LW) radiative effect. The LW cooling near cloud top produces a more saturated environment and a stronger dynamical circulation while cloud-base radiative warming of the upper layer creates the stability gap between the two cloud layers. Both cloud layers are sensitive to ice-forming nuclei number concentration since ice-phase microphysics provides a strong sink of cloud liquid water mass.